Final Draft
of the original manuscript:

Zhang, Y.; Tian, Z.; Zhao, X.; Li, N.; Haramus, V.M.; Yin, P.; Zou, A.:
Dual-modified bufalin loaded liposomes for enhanced tumor targeting.
In: Colloids and Surfaces A. Vol. 571 (2019) 72 - 79.
First published online by Elsevier: 21.03.2019

https://dx.doi.org/10.1016/j.colsurfa.2019.03.060

Dual-modified Bufalin loaded liposomes for enhanced tumor targeting

Yongchao Zhang[a#], Zhenfen Tian[a#], Xiaotong Zhao[a], Na Li[b], Vasil M. Garamus[c],

Peihao Yin*[d], Aihua Zou*[a]

[a]Shanghai Key Laboratory of Functional Materials Chemistry, State Key Laboratory of Bioreactor Engineering and Institute of Applied Chemistry, School of Chemistry and Molecular Engineering, East China University of Science and Technology, Shanghai 200237, P. R. China

[b]National Center for Protein Science Shanghai and Shanghai Institute of Biochemistry and Cell Biology, Shanghai 200237, P. R. China

[c]Helmholtz-Zentrum Geesthacht, Centre for Materials and Coastal Research, D-21502 Geesthacht, Germany

[d]Department of General Surgery, Putuo Hospital, Shanghai University of Traditional Chinese Medicine, 200062, P.R. China

*To whom correspondence should be addressed.

Tel/Fax.: +86-21-64252231

E-mail: aihuazou@ecust.edu.cn（AH Zou, yinpeihao1975@hotmail.com (PH Yin)

†East China University of Science and Technology (AH Zou), and Putuo Hospital (PH Yin).

The first two authors contribute equally to this article, they are co-first authors.

Abstract

Bufalin, a traditional oriental medicine, has been incorporated into liposomes for better targeting drug delivery. Bufalin-loaded liposome (L-BF), bufalin-loaded PEGylated liposome (L-PEG-BF) and bufalin-loaded RGD targeted PEGylated liposome (L-RGD-PEG-BF) were successfully developed with homogeneous particle size and sufficient physical stability in 30 days. The entrapment efficiency (EE) and drug loading efficiency (DL) of bufalin in these liposomes were about 85.4-90.6 % and 6.0-6.6 %, respectively. The morphologies of these liposomes were determined as small unilamellar vesicles by the measurements of transmission electron microscopy (TEM) and small angle X-ray scattering (SAXS). L-BF, L-PEG-BF and L-RGD-PEG-BF exhibited improved anticancer efficacy compared to free bufalin. Moreover, L-RGD-PEG-BF showed higher inhibition on the proliferation of A549 cells than the other two non-targeted bufalin liposomes in cytotoxicity study, and the growth inhibition concentration (IC_{50}) of L-RGD-PEG-BF (8.62±0.74 ng/mL) was much lower than pure bufalin (20.37±2.31 ng/mL). Both confocal and apoptosis assay indicated that L-RGD-PEG-BF was easier to be taken into cancer cells than non-targeted bufalin liposomes. Therefore, L-RGD-PEG-BF is expected to be an effective drug carrier for bufalin delivery in tumor treatment.

Key words: RGD peptide; Liposome; Bufalin; PEG; Active targeted ligand

1.Introduction

Bufalin, a traditional Chinese medicine obtained from the skin and parotid venom glands of the toad *Bufo bufo gargarizans cantor* or *Bufo melanostictus* [1-3], has significant anticancer activity against a broad spectrum of tumors, such as lung cancer [4], colon cancer [5], pancreatic cancer [6], and hepatocellular carcinoma [7]. However, the high toxicity, poor water solubility and short half-life of bufalin [8] have largely limited its potential application in cancer therapy. In order to overcome these drawbacks, many researchers have focused on the delivery systems of bufalin for treatment of tumor. Tian et al. [9] loaded bufalin into the nanoparticles consisted of biotinylated chitosan with entrapment efficiency of (77.5 ± 2.5) %. Hu et al. [10] prepared bufalin-loaded nanoparticles with pluronic polyetherimide using a thin film method with encapsulation efficiency of 75.71%. Liu et al. [11] developed a novel tumor-targeting polymeric prodrug of bufalin, P(OEGMA-co-BUF-co-Oct), exhibited improved anticancer efficacy against breast cancer. Considering that the complicated synthesis process and high costs, efforts are currently underway to investigate a simpler drug delivery for bufalin with high drug entrapment efficiency. Compared with those drug carriers, liposomal delivery systems have many advantages in the clinical application of anticancer, including the affinity to biological membrane, the size control property, and the loading capacity for both hydrophilic and hydrophobic drugs [12].

While conventional liposomes could rapidly clearance from the blood due to the adsorption of plasma proteins to the phospholipid membrane, which limited its application [13]. To solve this problem, surface modification and functionalization of the conventional liposome is necessarily.

PEGylated liposomes could prolong the circulation time in biological fluids through decrease the recognition of reticuloendothelial system [14], and also have the ability to passively accumulate in tumor tissues through Enhanced Permeability and Retention (EPR) effects [15]. Yuan et al. [16] prepared bufalin-loaded PEGylated liposomes with the mean particle size of 127.6 nm and the entrapment efficiency of 76.31%, and demonstrated that the solubility, the antitumor efficacy, and the pharmacokinetics of bufalin-loaded PEGylated liposomes were improved compared with those of bufalin entity. However, the following problem, such as the steric hindrance of PEGylation reduce the interactions between drug delivery and cancer cells, which result in the improper cellular uptake as well as the poor endosomal escape [17-20]. To overcome the above drawbacks related to “passive targeting”, “active targeting” was developed in present work by using RGD peptide (Ary-Gly-Asp). RGD peptide is often considered as an active targeting ligand, owing to its affinity for the αvβ3 integrin, which is overexpressed on the neovascular endothelial cells of tumor proliferating, while minimally expressed on normal tissues [21-23].

In this study, we aimed at constructing stable liposome composition for bufalin with an appropriate size, high drug loading, long-circulation time and tumor-targeted function. DSPE-PEG (2000)-Maleimide and DSPE-PEG (2000)-RGD were synthesized and then incorporated into the liposome system to obtain bufalin loaded long-circulating PEGylated liposome (L-PEG-BF) and RGD-targeted PEGylated liposome(L-RGD-PEG-BF). The samples were characterized by dynamic lights scattering (DLS), TEM and SAXS measurements. The cellular uptake, *in vitro* cytotoxicity and apoptosis studies were performed to observe the physiological effect of the RGD peptid-modified bufalin carrier.

2. Materials and methods

2.1 Materials

Hydrogenated soya phosphatidylcholine (HSPC) was purchased from Lipoid (Ludwigshafen, Germany). Cholesterol (CHOL) (>98%), 1, 2-distearoyl-*sn*-glycero-3-phosphoethanolamine-N-[methoxy (polyethylene glycol)-2000] [DSPE-mPEG (2000)], and 1, 2-distearoyl-*sn*-glycero-3-phosphoethanolamine-N-[maleimide (polyethylene glycol)-2000] (DSPE-PEG (2000)-mal) were obtained from Avanti Polar Lipids (Alabaster, AL). RGD peptide (sequence: H-Gly-Ary-Gly-Asp-Ser-Pro-Cys-OH, molecule weight, 690.73 Da) was purchased from NJPeptide Biotechnology Inc (Nanjing, China). Rhodamine B (RB) (RB ≥99%) and bufalin were purchased from Acros Organics (USA) and Chengdu Herbpurify Co. Ltd. (Chengdu, China) respectively. Double distilled water.

2.2 Synthesis of DSPE-PEG (2000)-RGD

DSPE-PEG (2000)-RGD was prepared according to the method reported by Rivest V with a slight modification [24] (Fig. S1). Briefly, DSPE-PEG (2000)-Mal and RGD peptide were dissolved in a phosphate buffer solution (PBS, pH=7.4) respectively. After stirred overnight in a glass bottle at 4 ºC, the mixed solution was dialyzed by using a dialysis membrane (MWCO=1000 kDa) to remove the excess RGD peptide. The obtained product was identified by matrix-assisted laser desorption/ionization time-of-flight (MALDI-TOF) mass spectrometry (AB SCIEX 4800 Plus MALDI TOF/TOF™ Analyzer, America).

2.3 Liposome Preparation

L-BF was prepared by a modified ethanol injection method [25]. In detail, a certain of bufalin, HSPC and CHOL were dissolved in 10 mL of ethanol and placed in a flask. Then the ethanol solution was slowly injected into PBS buffer (pH=7.4, 55 ºC). The mixture was magnetically stirred at 55 ºC until the ethanol was completely removed. At last, the product was under ultrasound for 5 minutes. The L-PEG-BF and L-RGD-PEG-BF were prepared the same as described above except adding DSPE-mPEG

(2000) and DSPE-PEG (2000)-RGD into the flask, respectively. Fluorescent liposomes (L-RB, L-PEG-RB and L-RGD-PEG-RB) were prepared according to the above method but the bufalin was replaced by RB [26].

2.4 Dynamic Lights scattering

The mean hydrodynamic diameter, polydispersity (PDI) and zeta potential were determined by dynamic lights scattering spectrophotometry (Delsa™ Nano C Particle Analyzer, Beckman Coulter, USA) at 25 ºC with an angle of 165º. The liposomes were measured at certain interval (after 1, 7, 15, 30 days). Each test was performed for three times.

2.5 Entrapment Efficiency and Drug Loading

Centrifugal-ultrafiltration method was used to determine the entrapment efficiency of the bufalin in L-BF, L-PEG-BF, L-RGD-PEG-BF. 500μL of the prepared liposomes were loaded into the upper chamber of a centrifuged tube matched with an ultrafilter (Pall Corp, Port Washington, NY; MWCO=10 kDa), which was centrifuged at 8000rpm at 4 ºC for 40 min. Then the un-entrapped BF and the dispersion medium were separated into the ultrafilter. After separation, the filtrate was diluted by PBS (pH=7.4) and the amount of free bufalin (W_{BF}) was measured by a UV–vis spectrophotometer (Evolution 220, Thermo Fisher Scientific, USA) at 298 nm. The standard curve of BF concentration at 298 nm was y = 0.01226x + 0.01194 (R^2 = 0.99932) which was resulted in a linear regression.

The entrapment efficiency (EE%) and drug loading (DL%) was calculated according to the following equations [27]:

$$EE\ (\%) = (W_T - W_{BF}) / W_T \times 100\ \% \quad (1)$$

$$DL\ (\%) = (W_T - W_{BF}) / W_L \times 100\ \% \quad (2)$$

Where the W_T was the total amount of BF added into the liposome, W_L represented the total amount of lipid and W_{BF} was the amount of un-loaded BF.

2.6 Liposomes morphology

For TEM studies, the samples were firstly drop on a Formvar-copper grid (Science Services, Munchen) and air-dried for 20 min at room temperature. Then the liposomes were stained with sodium phosphotungestic acid 2 % (w/v) for 15s at room temperature and imaged on a TEM (JEOL-1400, Jeol, Tokyo, Japan).

2.7 Small angle X-ray scattering

SAXS experiments were carried out at beamline BL19U2 of National Center for Protein Science Shanghai (NCPSS) at Shanghai Synchrotron Radiation Facility (SSRF). The measurement λ of X-ray radiation was 1.033 Å. The detecting range of momentum transfer $q=4\pi \sin/\lambda$, where 2θ is the scattering

angle was set as 0.01-0.5 $Å^{-1}$ corresponding to investigated length scale from 10 to 600 Å. The flow cell is a cylindrical quartz capillary with diameter of 1.5 mm and wall thickness of 10 μm and the exposure time was set to 1-2 seconds in order to reduce the radiation damage. Ten imagines were taken for each sample by a Pilatus 1M detector (DECTRIS Ltd) to obtain good signal-to-noise ratios. By using the software package BioXTAS RAW, 1-D SAXS curves were obtained.

2.8 In vitro drug release studies

The *in vitro* release experiments of bufalin from liposomes were performed by dialysis method. Briefly, a 3 mL aliquot of each liposome solution was placed into cellulose membrane dialysis tubes (MWCO = 8000-12000 Da). Then the dialysis tubes with liposomes were immersed into 100 mL release medium (PBS, pH=7.4) at (37±0.5) °C for 3 days in a rotary shaker with thermos tatted bath. 3 mL samples were removed from release medium at predesigned interval and an equal volume of fresh PBS with same pH and temperature were added into release medium. The concentration of released bufalin was determined by UV-vis spectrophotometer (UV-1800; Shimadzu, Japan) at 298 nm. Each sample was measured three times.

2.9 Cell culture

A549 cancer cells, one kind of human lung cancer cell lines were cultured by F12K medium supplemented with 10 % fetal bovine serum (FBS) and penicillin (100 U/mL) (Invitrogen, Carlsbad, CA, USA). The cells were placed into petri dishes with a humidified 5% CO_2 atmosphere at 37 °C. The A549 cell line was purchased from American Type Culture Collection (Manassas, VA, USA). The culture medium was replenished every day.

2.10 In vitro cytotoxicity assay

The *in vitro* cytotoxicity of the liposomes was evaluated by Cell Counting Kit (CCK) tests, which is a high-sensitive cell proliferation and cytotoxicity detection kit based on WST – 8 (2 - (2 – methoxy – 4 - nitrophenyl) – 3 - (4 - nitrophenyl)- 5 - (2, 4 - disulfoanilino) - 2H - tetrazolium monosodium salt). A549 cells were seeded into 96-well plats with 5×10^3 cells and 100μL medium per well and then incubated for 24 h. The cancer cells were exposed to a series of concentrations of pure BF, L-BF, L-PEG-BF and L-RGD-PEG-BF at 37 °C. After 48 h, 10μL CCK-8 was added into per well and then the cells were incubated for 1 h. At last, the absorbance was measured at 450 nm by using an enzyme-linked immunosorbent assay (Infinite F200, TECAN, Switzerland). The cell viability was expressed as percentage and untreated A549 cells were taken as 100% viable.

2.11 In vitro cell uptake study

For *in vitro* liposomes cell uptake assay, A549 cells were placed into 6-well plats at s density of

3×10^5 cells per well and incubated with L-RB, L-PEG-RB and L-RGD-PEG-RB for 4 h at 37 °C. Then the medium was removed and the cells were washed with PBS for three times. The cell uptake images were visualized and photographed by a laser scanning confocal microscope (TCS-SP8, Germany).

2.12 Apoptosis analysis

A549 cancer cells were seeded in 6-well plats for 24 h and then exposed to certain concentration of L-BF, L-PEG-BF and L-RGD-PEG-BF, respectively. After incubated for 48 h, the cells were placed into flow tubes and washed with cold PBS for twice. 100 μL buffer (10×), 5 μL FITC and 5 μL PI was added into the flow tubes. Next, the tubes were placed in dark for 15 min and added 400 μL buffer (10×). Finally, the fluorescence of the liposomes was detected by a flow cytometer (JAZZ, USA) within 1h.

3. Results and discussion

3.1 Liposomes preparation and characterization

In order to obtain the stable liposome formulations for BF with better EE and DL values, 5 samples with different drug/lipid ratios were prepared as shown in Table S1. The DL values of BF raised with the increase of the drug/lipid ratio, while the EE values of BF increased initially and then decreased when the ratio of drug/lipid reached 1/10. Taking the above observation into account, sample 2 with the ratio of BF/HSPC (w/w) at 1:10 has better DL and EE values, which was chosen as the optimal formulations for further investigation.

DSPE-mPEG (2000) and DSPE-PEG (2000)-RGD were successfully synthesized (Fig. S2) for the preparation of BF loaded long-circulating liposomes and RGD peptide targeted PEGylated liposomes. Then L-PEG-BF and L-RGD-PEG-BF were prepared with the same method except adding DSPE-mPEG (2000) and DSPE-PEG (2000)-RGD into the liposome system.

As can be seen from Fig.1, the EE values of L-BF, L-PEG-BF and L-RGD-PEG-BF were (85.4±1.58) %, (90.4±3.58) % and (90.6±4.98) %, respectively. The EE values of L-PEG-BF and L-RGD-PEG-BF were higher than that of L-BF, which indicated more bufalin were entrapped in the PEGylated liposome or the RGD-targeted PEGylated liposome than in the conventional liposome [28]. It was noteworthy that the DL value of L-BF (6.6%) was slightly higher than the other two samples, which was due to the increase of the total amount of lipids in the other two samples. With time going, the EE and DL values of L-BF reduced much more quickly than that of the other two (Fig.1). On the basis of these results, it can be concluded that the DSPE-mPEG (2000) and DSPE-PEG (2000)-RGD were more beneficial to the encapsulation of bufalin in liposomes. Yin et al. have reported the loading of bufalin with mPEG-PLGA-PLL-cRGD nanoparticles, in which the EE value was (81.7±0.89) % and the DL value was (3.92±0.16) % [29]. Compared with the EE and DL values of bufalin reported from the references, it is

obvious that the obtained L-BF, L-PEG-BF and L-RGD-PEG-BF in present work are superior.

As shown in Fig. 2, the mean particle size of L-PEG-BF and L-RGD-PEG-BF were determined as 89.5±4.7 nm and 87.9±3.9, respectively, which were much smaller than that of L-BF (215.1±2.3) nm. The addition of PEG and RGD resulted more homogeneous particle compared with L-BF [30]. The PDI value of the liposomes was on behalf of the homogeneous degree [31]. From Fig.2, it can be seen that the PDI value of L-BF was about 0.25, and both the PDI values of L-PEG-BF and L-RGD-PEG-BF were approximately 0.20. The mean particle sizes and PDI values of all liposomes remained almost unchanged for 30 days, which indicated that L-BF, L-PEG-BF and L-RGD-PEG-BF had good stability during the storage.

Zeta potential could characterize the surface charge of the liposome, which was an important indication for the stability of the colloid nanoparticle systems [32]. As shown in Fig.2, the zeta -potential values of L-BF, L-PEG-BF and L-RGD-PEG-BF exhibited negative charges on the liposome surfaces, which might be caused by the overall negative charge of HSPC. All samples exhibited a stable potential approximately -19 to -21 mV, although the minor changes on zeta potential values during storage, which indicated that L-BF, L-PEG-BF and L-RGD-PEG-BF exhibited good stability for at least 30 days. This result is consistent with the above results obtained from PDI values and mean particle size.

The morphologies of bufalin loaded liposomes were detected by TEM. From Fig.3, it is obvious that L-BF, L-PEG-BF and L-RGD-PEG-BF all present the small unilamellar vesicles (SUVs) with uniquely recognizable phospholipid bilayers of the vesicle membrane. In addition, all the samples were spherical morphology with part of overlap. The similar characters of L-BF, L-PEG-BF and L-RGD-PEG-BF displayed in Fig.3 demonstrated that the incorporation of DSPE-mPEG (2000) and DAPE-PEG (2000)-RGD did not obviously affect the morphology of the liposomes. The sizes of L-BF were about 99.64-161.25 nm, while L-PEG-BF and L-RGD-PEG-BF have relatively more uniform particle size of about 70.64-125.10 nm and 65.54-107.58 nm, respectively. The dehydrated sizes for L-BF, L-PEG-BF and L-RGD-PEG-BF measured by TEM was smaller than the hydrodynamic diameter measured by DLS, which could be ascribed to shrinkage after being dried during sample preparation for the TEM measurements [33].

SAXS was used to get the mean or global features of the samples since TEM can image only a small part of the bulk volume. Representative SAXS curves, before and after the BF loading for the conventional liposome, PEGylated liposome and RGD targeted PEGylated liposome were shown in Fig. 4. All of the SAXS curves showed no significant quasi-Bragg peaks and only broad maximum. This diffraction patterns were exhibited as uncorrelated bilayers, such as unilamellar and/or few layer vesicles

[34], which was similar with the results of TEM. Moreover, for polydisperse systems, the absence of the peaks was caused by the superposition of many different vesicle sizes and thickness, which demonstrated that there were no multilamellar vesicles or other periodically nanoparticles, such as cubosomes [30]. From Fig. 4, it can be seen that the SAXS intensity of L-PEG and L-RGD-PEG were higher than that of blank liposome (Blank-L) and the SAXS intensity of L-BF, L-PEG-BF and L-RGD-PEG-BF were different from their corresponding blank liposomes.

SAXS data show significant increasing of scattering intensity at lowest q range i.e., Guinier´s regime of scattering behavior I(q) ~ exp ($-q^2Rg^2/3$) was not achieved by present SAXS set up (Rg is radius gyration of scattering contrast). It meant that whole particle (vesicle) was not visible in performed scattering experiments and it was possible to get information about structure of internal parts of vesicles or overall size indirectly. The scattering of the vesicle in which radius was much larger than layer thickness could be written as [35]:

$$I(q) \sim (R^2\{sin(qR)/(qR)\}\{ sin(qT)/q\})^2 \qquad (3)$$

where R and T are the vesicle radius and thickness, respectively.

The observed minimum at scattering curve was connected with 0 values of sin(qT) and suggested (Fig. 4A) that the thickness of vesicles (movement to low q) and polydispersity (vanishing of sharpness of minimum) increased for RGD targeted PEGylated liposome. Corresponding loading with BF (Fig. 4B-D) led to different effects the vesicles became less polydisperse.

In order to get structural information such as a distribution of scattering length density along the smaller dimension, Indirect Fourier Transformation (IFT) analysis in approximation of infinitely thin objects has been applied [36]. The thickness pair distance distribution function $p_T(r)$ describe the scattering intensity via:

$$I(q) = \frac{2\pi^2}{q^2}\int_0^\infty p_T(r)\cos(qr)\,dr \quad . \qquad (4)$$

The $p_T(r)$ function was connected with the distribution of the scattering contrast between object and solvent. IFT satisfactorily describes our experimental data (solid lines in Figure 4). The $p_T(r)$ functions were shown in Fig. S3. The negative values of $p_T(r)$ in the intermediate *r*-range could be explained by different sign of the scattering contrast for alkyl chains (positive) and polar groups (negative) of lipid in water. After determination of the pair distance distribution function, the mass per unit area of the aggregate M_S and the radius of gyration of the cross section of the bilayer $R_{T,g}$ has been calculated and presented in Table S2.

p(r) functioned show number of minima and maxima with maximal thickness up to 150 Å which suggested the formation of 3-4 layers vesicles (thickness of one bilayer is around 30 Å). PEGylation an

RGD targeting of PEGylated vesicles lead to slight increasing of radius of gyration of thickness. Adsorption of BF took place in different way i.e., for Blank-L and L-PEG the adsorption led to slightly increase of radius of gyration of thickness (BF located in peripheric of vesicle layer) and for L-RGD-PEG it has opposite effect and here we could assume that BF was incorporated inside of vesicle layer.

3.2 In vitro bufalin release studies

The profiles of bufalin released from the PEGylated liposome and the RGD-targeted PEGylated liposome were carried out by using the dialysis method in a medium of PBS buffer (pH=7.4) at (37±0.5) °C. As controls, bufalin released from pure BF solution and L-BF was also investigated. As shown in Fig.5, more than 95% of bufalin was released from the pure BF solution within 10h and the accumulative value reached 100% in the following two hours. L-BF showed a relatively slower drug release, approximately (81.05±3.06) % and (97.81±0.21) % of bufalin was released after 10h and 72h. In contrast, the release values of bufalin from L-PEG-BF and L-RGD-PEG-BF were (51.69±1.77) % and (44.69±1.89) % within 10h, respectively. Moreover, the accumulative release values of L-PEG-BF and L-RGD-PEG-BF were (84.21±0.31) % and (80.29±1.23) % until 72h, respectively. The *in vitro* release of bufalin from both L-PEG-BF and L-RGD-PEG-BF liposomes was significantly lower than that of conventional liposome, which meant that PEG chain could be more effective to prolong the release of bufalin [37]. This result was also consistent with the results from TEM and SAXS experiments, which further confirmed that both DSPE-mPEG (2000) and DSPEG-PEG (2000)-RGD were successfully incorporated into the liposomes.

3.3 Biological activity of bufalin in A549 cell

In vitro cytotoxicity assay was carried out to evaluate the activity of BF loaded liposomes on the cancer cells by using the CCK-8 assay. Blank-RGD-PEG-L and pure BF were also applied to cancer cells with the same procedures detected as controls. Fig.6 displayed the viability of human lung cancer cells (A549) treated with different concentrations (0-100 ng/mL) of Blank-RGD-PEG-L, BF, L-BF, L-PEG-BF and L-RGD-PEG-BF. The viability of A549 cells treated with 6.25 ng/mL and 100 ng/mL pure BF were (96.6±3.7) % and (21.01±3.2) %, respectively. Compared with pure BF, the cytotoxicity of L-BF against A549 cancer cells at the same concentration was slightly higher than that of free BF. While L-PEG-BF showed much more significant inhibition against the proliferation of A549 cells, with only (13.21±3.5) % of cell viability at the concentration of 100 ng/mL. This indicated that modified with DSPE-mPEG (2000) on the surface of the liposome prolonged the release of BF from the liposome. It is obvious that L-RGD-PEG-BF possessed best inhibition potential than the other three samples at a concentration ranging from 6.25 ng/mL to 100 ng/mL. The cell viability at the concentration of 100 ng/mL of

L-RGD-PEG-BF was only (10.11±2.2) %. A possible explanation is that the RGD peptide can be specifically binding on $\alpha_v\beta_3$ integrin which is existed in A549 cells [38]. It should be noted that the Blank-RGD-PEG-L (0-100 ng/mL) did not show any cytotoxicity against A549 cells after 48 h incubation.

Table S3 showed the growth inhibition concentration (IC_{50}) of BF, L-BF, L-PEG-BF, and L-RGD-PEG-BF. The IC_{50} values of BF aqueous solution, L-BF and L-PEG-BF were (20.37±2.31) ng/mL, (18.36±1.06) ng/mL and (13.58±1.83) ng/mL, respectively. While the IC_{50} value of L-RGD-PEG-BF was (8.62±0.74) ng/mL, which was 2.36 times lower than that of free BF. These results suggested that the RGD peptide targeted PEGylated liposomes were more effective than non-targeted liposomes and pure BF.

The cell uptake of liposomes plays a significant role in their application as a drug carrier. In this study, the uptake of RB loaded in conventional liposome, L-PEG, and L-RGD-PEG by A549 cells was analyzed by confocal microscope. The fluorescence intensity was proportional to the amount of RB internalized by the cells. As shown in Fig.7A, the uptake image of L-RB showed slightly fluorescent intensity, which indicated that few L-RB was taken into A549 cells after incubated for 6 h. Fig.7B showed the cells uptake image of L-PEG-RB, where the fluorescent intensity became obvious. Compared to Fig.7B, Fig.7C showed much stronger fluorescent intensity which demonstrated that the uptake of L-RGD-PEG-RB into cancer cells were much easier. These results were also in good consistent with that of *in vitro* cytotoxicity assay.

The bioactivity of bufalin-loaded liposomes on A549 cells was further studied by the flow cytometry [39]. The A549 cells were exposed to free BF, L-BF, L-PEG-BF and L-RGD-PEG-BF for 48 h and stained with FITC Annexin V Apoptosis Detection Kit I, then examined by flow cytometer. Fig.8 displayed the percentage of cell population against different medium of apoptosis. As shown in Fig.8, A549 cell apoptosis of free BF and L-BF were no obvious difference after cultured for 48 h, which were 9.46% and 10.99% of total apoptosis respectively. During the same time period, A549 cells apoptosis of L-PEG-BF were 11.83% at the early stage and 28.11% at the late stage. While for L-RGD-PEG-BF, the cell apoptosis rate increased to 20.99% and 46.70%, respectively. The above results indicated that L-RGD-PEG-BF was much easier to be taken into cancer cells, which were consistent with those obtained from *in vitro* cytotoxicity and uptake assays.

4. Conclusion

Three liposome systems (L-BF, L-PEG-BF, L-RGD-PEG-BF) were successfully developed using a

modified ethanol injection method in present work. All samples of L-BF, L-PEG-BF and L-RGD-PEG-BF exhibited small unilamelar vesicles with high entrapment efficiency and a good colloidal stability during the storage. L-PEG-BF and L-RGD-PEG-BF exhibited the obvious prolonged-release property. Noteworthily, L-RGD-PEG-BF showed an active targeting property on A549 cells. The enhancement of cytotoxicity and the number of apoptotic cancer cells exhibited by L-RGD-PEG-BF were higher than that of non-targeted liposomes and free BF. Consistently, L-RGD-PEG-BF showed a much higher cellular uptake than non-targeted liposome and free BF, which may be attributed to the affinity of RGD peptide with αvβ3 integrin overexpressed on the tumor cells. As can be seen that this liposome nanotechnology demonstrated considerable potential for translation in Chinese medicine. Therefore, *in vivo* evaluations of L-RGD-PEG-BF should be the next rational extension of this work.

Acknowledgment

We gratefully acknowledge the support of this work by the National Natural Science Foundation of China (Grant No. 21573070), the National Natural Science Foundation of China (Grant No. 21872051). We thank the staff of the BL19U2 beamline at the National Center for Protein Science Shanghai and the Shanghai Synchrotron Radiation Facility for assistance during data collection.

References

[1] L. Krenn, B. Kopp, Bufadienolides from animal and plant sources, Phytochemistry. 48(1) (1998) 1-29

[2] F.H. Qi, A.Y. Li, Y. Inagaki, N. Kokudo, S. Tamura, M. Nakata, W. Tang, Antitumor activity of extracts and compounds from the skin of the toad Bufo bufo gargarizans Cantor, International Immunopharmacology. 11(3) (2011) 342-349

[3] N. Takai, N Kira, T. Ishii, T. Yoshida, M. Nishida, Y. Nishida, K. Nasu, H Narahara, Bufalin, a traditional oriental medicine, induces apoptosis in human cancer cells, Asian Pac J Cancer Prev. 13 (2012) 399-402

[4] Y.T. Jiang, Y. Zhang, J.L. Luan, H.Y. Duan, F. Zhang, K. Yagasaki, G.Y. Zhang, Effects of bufalin on the proliferation of human lung cancer cells and its molecular mechanisms of action, Cytotechnology. 62(6) (2010) 573-583

[5] C.M. Xie, W.Y. Chan, S. Yu, J. Zhao, C.H.K. Cheng, Bufalin induces autophagy-mediated cell death

in human colon cancer cells through reactive oxygen species generation and JNK activation, Free Radical Biol Med. 51(7) (2011) 1365-1375

[6] M.Y. Li, X.J. Yu, H. Guo, L.M. Sun, A.J. Wang, Q.J. Liu, X.W. Wang, J.S. Li, Bufalin exerts antitumor effects by inducing cell cycle arrest and triggering apoptosis in pancreatic cancer cells, Tumor Biology. 35(3) (2014) 2461-2471

[7] D.Z. Qiu, Z.J. Zhang, W.Z. Wu, Y.K. Yang, Bufalin, a component in Chansu, inhibits proliferation and invasion of hepatocellular carcinoma cells, BMC Complement Altern Med. 13(1) (2013) 185

[8] Z. Yang, Y. Teng, H. Wang, H.M. Hou, Enhancement of skin permeation of bufalin by limonene via reservoir type transdermal patch: formulation design and biopharmaceutical evaluation, Int J Pharm. 447(1) (2013)231-240

[9] X. Tian, H.Z. Yin, S.C. Zhang, Y. Luo, K. Xu, P. Ma, C.G. Sui, F.D. Meng, Y.P. Liu, Y.H. Jiang, J. Fang, Bufalin loaded biotinylated chitosan nanoparticles: An efficient drug delivery system for targeted chemotherapy against breast carcinoma, European Journal of Pharmaceutics and Biopharmaceutics. 87(3) (2014) 445-453

[10] Q. Hu, B. Liang, Y. Sun, X.L. Guo, Y.J. Bao, D.H. Xie, M. Zhou, Y.R. Duan, P.H. Yin, Z.H. Peng, Preparation of bufalin-loaded pluronic polyetherimide nanoparticles, cellular uptake, distribution, and effect on colorectal cancer, International journal of nanomedicine. 9 (2014) 4035-4041

[11] T. Liu, T.T. Jia, X. Yuan, C. Liu, J. Sun, Z.H. Ni, J. Xu, X.H. Wang, Y. Yuan, Development of octreotide-conjugated polymeric prodrug of bufalin for targeted delivery to somatostatin receptor 2 overexpressing breast cancer in vitro and in vivo, International journal of nanomedicine. 11 (2016) 2235-2250

[12] H.K. Han, H.J. Shin, D.H. Ha, Improved oral bioavailability of alendronate via the mucoadhesive liposomal delivery system, European Journal of Pharmaceutical Sciences. 46(5) (2012) 500-507

[13] H. Daraee, A. Etemadi, M. Kouhi, S. Alimirzalu, A. Akbarzadeh, Application of liposomes in medicine and drug delivery. Artificial Cells, Nanomedicine, and Biotechnology. 44(1) (2016) 381-391

[14] T.M. Allen, P.R. Cullis, Liposomal drug delivery systems: From concept to clinical applications, Advanced Drug Delivery Reviews. 65(1) (2013) 36-48

[15] E.A. Forssen, D.M. Coulter, R.T. Proffitt, Selective in vivo localization of daunorubicin small unilamellar vesicles in solid tumors, Cancer Res. 52 (1992) 3255–3261

[16] J.N. Yuan, X.X. Zhou, W. Cao, L.L. Bi, Y.F. Zhang, Q. Yang, S.W. Wang, Improved Antitumor Efficacy and Pharmacokinetics of Bufalin via PEGylated Liposomes, Nanoscale Research Letters. 12(1) (2017) 585

[17] A.L.B. Seynhaeve, B.M. Dicheva, S. Hoving, G.A. Koning, T.L.M. ten Hagen, Intact Doxil is taken up intracellularly and released doxorubicin sequesters in the lysosome: Evaluated by in vitro/in vivo live cell imaging, Journal of Controlled Release. 172(1) (2013) 330-340

[18] Y.L. Tseng, J.J. Liu, R.L. Hong, Translocation of Liposomes into Cancer Cells by Cell-Penetrating Peptides Penetratin and Tat: A Kinetic and Efficacy Study, Molecular Pharmacology. 62(4) (2002) 864

[19] H. Hatakeyama, H. Akita, K. Kogure, M. Oishi, Y. Nagasaki, Y. Kihira, M. Ueno, H. Kobayashi, H. Kikuchi, H. Harashima, Development of a novel systemic gene delivery system for cancer therapy with a tumor-specific cleavable PEG-lipid, Gene Ther. 14 (2007) 68–77

[20] H. Hatakeyama, H. Akita, H. Harashima, A multifunctional envelope type nano device (MEND) for gene delivery to tumours based on the EPR effect: a strategy for overcoming the PEG dilemma, Adv. Drug. Deliv. Rev 63 (2011) 152–160

[21] J. Nicolas, S. Mura, D. Brambilla, N. Mackiewicz, P. Couvreur, Design, functionalization strategies and biomedical applications of targeted biodegradable/biocompatible polymer-based nanocarriers for drug delivery, Chemical Society Reviews. 42(3) (2013)1147-1235

[22] C. Kumar, Integrin αvβ3 as a Therapeutic Target for Blocking Tumor-Induced Angiogenesis, Current Drug Targets. 4(2) (2003) 123-131

[23] Z.M. Guo, B. He, H.W. Jin, H.R. Zhang, W.B. Dai, L.R. Zhang, H. Zhang, X.Q. Wang, J.C. Wang, X. Zhang, Q. Zhang, Targeting efficiency of RGD-modified nanocarriers with different ligand intervals in response to integrin αvβ3 clustering, Biomaterials. 35(23) (2014) 6106-6117

[24] V. Rivest, A. Phivilay, C. Julien, S. Bélanger, C. Tremblay, V. Émond, F. Calon, Novel Liposomal Formulation for Targeted Gene Delivery, Pharmaceutical Research. 24(5) (2007) 981-990

[25] Y. Maitani, S. Igarashi, M. Sato, Y. Hattori, Cationic liposome (DC-Chol/DOPE=1:2) and a modified ethanol injection method to prepare liposomes, increased gene expression, International Journal of Pharmaceutics. 342(1) (2007) 33-39

[26] J. Wu, Q. Liu, R.J. Lee, A folate receptor-targeted liposomal formulation for paclitaxel, International Journal of Pharmaceutics. 316(1) (2006) 148-153

[27] Y. Liu, F.P. Gao, D. Zhang, Y.S. Fan, X.G. Chen, H. Wang, Molecular structural transformation regulated dynamic disordering of supramolecular vesicles as pH-responsive drug release systems, Journal of Controlled Release. 173 (2014) 140-147

[28] G. Kibria, H. Hatakeyama, N. Ohga, K. Hida, H. Harashima, Dual-ligand modification of PEGylated liposomes shows better cell selectivity and efficient gene delivery, Journal of Controlled Release. 153

(2011) 141-148

[29] P.H. Yin, Y. Wang, Y.Y. Qiu, L.L. Hou, X. Liu, J.M. Qin, Y.R. Duan, P.F. Liu, M. Qiu, Q. Li, Bufalin-loaded mPEG-PLGA-PLL-cRGD nanoparticles: preparation, cellular uptake, tissue distribution, and anticancer activity, International journal of nanomedicine. 7(2012) 3961-3969

[30] Y.Y. Chen, L.V. Minh, J.W. Liu, B. Angelov, M. Drechsler, V.M. Garamus, R. Willumeit-Römer, A.H. Zou, Baicalin loaded in folate-PEG modified liposomes for enhanced stability and tumor targeting, Colloids and Surfaces B: Biointerfaces. 140 (2016) 74-82

[31] C. Tan, S.Q. Xia, J. Xue, J.H. Xie, B. Feng, X.M. Zhang, Liposomes as Vehicles for Lutein: Preparation, Stability, Liposomal Membrane Dynamics, and Structure, Journal of Agricultural and Food Chemistry. 61(34) (2013) 8175-8184

[32] B. Heurtault, P. Saulnier, B. Pech, J.E. Proust, J.P. Benoit, Physico-chemical stability of colloidal lipid particles, Biomaterials. 24(23) (2003) 4283-4300

[33] W. Wu, Q.J. Zhang, J.T. Wang, M. Chen, S. Li, Z. F. Lin, J.S. Li, Tumor-targeted aggregation of pH-sensitive nanocarriers for enhanced retention and rapid intracellular drug release, Polymer Chemistry. 5(19) (2014) 5668-5679

[34] P. Georg, K. Richard, P.N. Beatriz, R. Michael, L. Karl, L. Peter, Structural analysis of weakly ordered membrane stacks, Journal of Applied Crystallograph. 36 (2003) 1378-1388

[35] J.S. Pedersen, Analysis of small-angle scattering data from colloids and polymer solutions: modeling and least-squares fitting, Advances in colloid and interface science. 70 (1997): 171-210

[36] O. Glatter, A new method for the evaluation of small- angle scattering data, Journal of Applied Crystallography.10 (1977) 415-421

[37] W.Y. Su, H.J. Wang, S. Wang, Z.Y. Liao, S.H. Kang, Y. Peng, L. Han, J. Chang, PEG/RGD-modified magnetic polymeric liposomes for controlled drug release and tumor cell targeting, International Journal of Pharmaceutics. 426 (2012) 170-181

[38] F.F. Wang, L. Chen, R. Zhang, Z.P. Chen, L. Zhu, RGD peptide conjugated liposomal drug delivery system for enhance therapeutic efficacy in treating bone metastasis from prostate cancer, Journal of Controlled Release. 196 (2014) 222-233

[39] X.L. Liu, M.T Han, J.W. Xu, S.C. Geng, Y. Zhang, X.H. Ye, J.X. Gou, T. Yin, H.B. He, X. Tang, Asialoglycoprotein receptor-targeted liposomes loaded with a norcantharimide derivative for hepatocyte-selective targeting, Int J Pharm. 520(1) (2017) 98-110

Figure Captions

Fig. 1 The EE and DLvalues of L-BF, L-PEG-BF and L-RGD-PEG-BF during 30 days

Fig. 2 Physical characterizations of L-BF, L-PEG-BF and L-RGD-PEG-BF: mean particle size, PDI and zeta potential

Fig. 3 The TEM images of L-BF (A), L-PEG-BF (B) and L-RGD-PEG-BF (C)

Fig. 4 SAXS curves of Blank-L, Blank-L-PEG and Blank-L-RGD-PEG (A) and the corresponding curves after BF loading: L-BF(B), L-PEG-BF(C) and L-RGD-PEG-BF(D)

Fig. 5 *In vitro* drug release curves of BF, L-BF, L-PEG-BF and L-RGD-PEG-BF in PBS at 37 °C

Fig. 6 *In vitro* cytotoxicity of BF, L-BF, L-PEG-BF and L-RGD-PEG-BF on A549 cells by CCK-8 assay (48 h)

Fig. 7 *In vitro* uptake images of L-RB (A), L-PEG-RB (B) and L-RGD-PEG-RB (C) in A549 cells by laser scanning confocal microscope

Fig. 8 Flow cytometry assay of apoptosis on A549 cells induced by BF (A), L-BF (B), L-PEG-BF (C) and L-RGD-PEG-BF (D)

Fig.1

Click here to download high resolution image

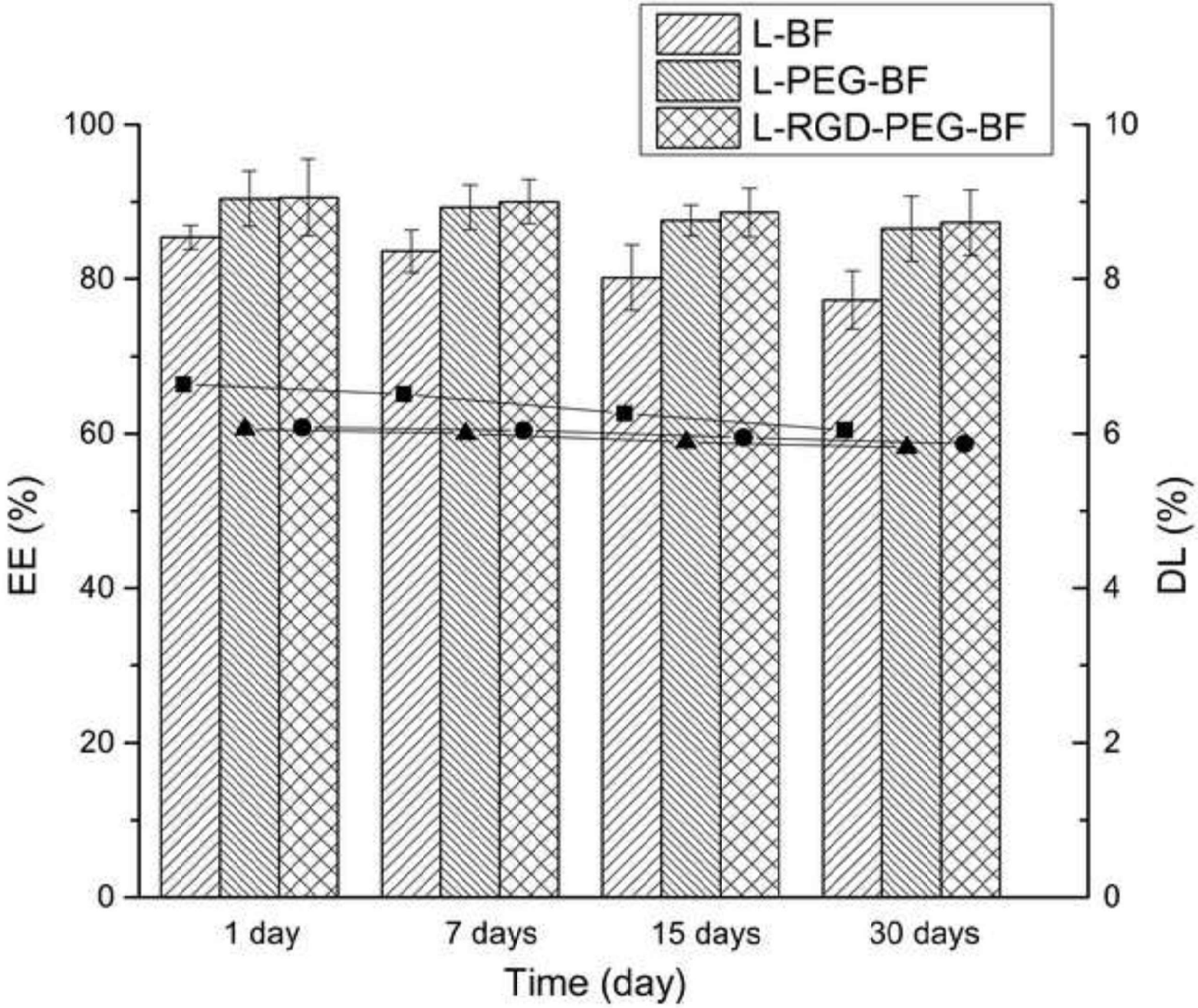

Fig.2

Click here to download high resolution image

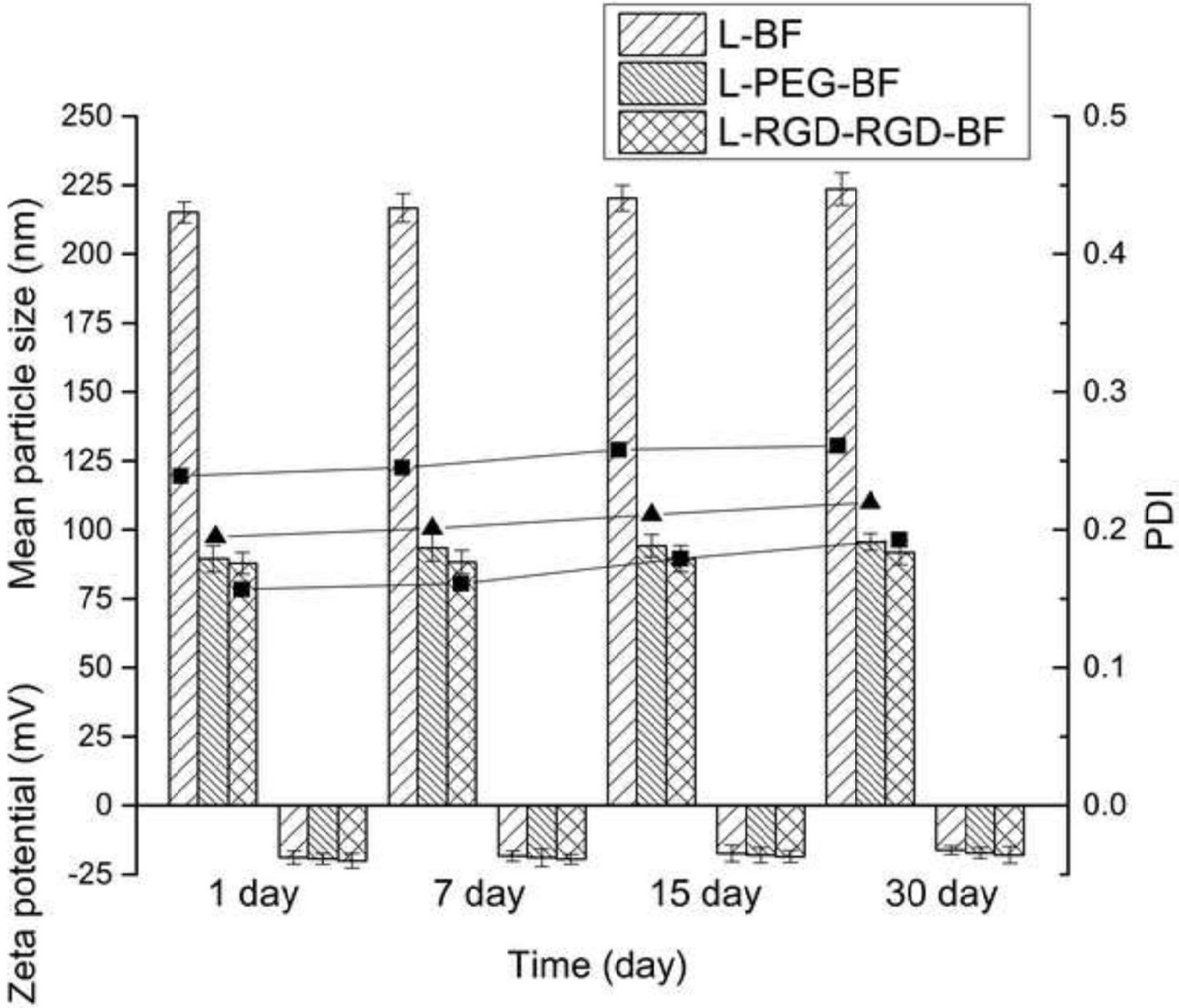

Fig.3

Click here to download high resolution image

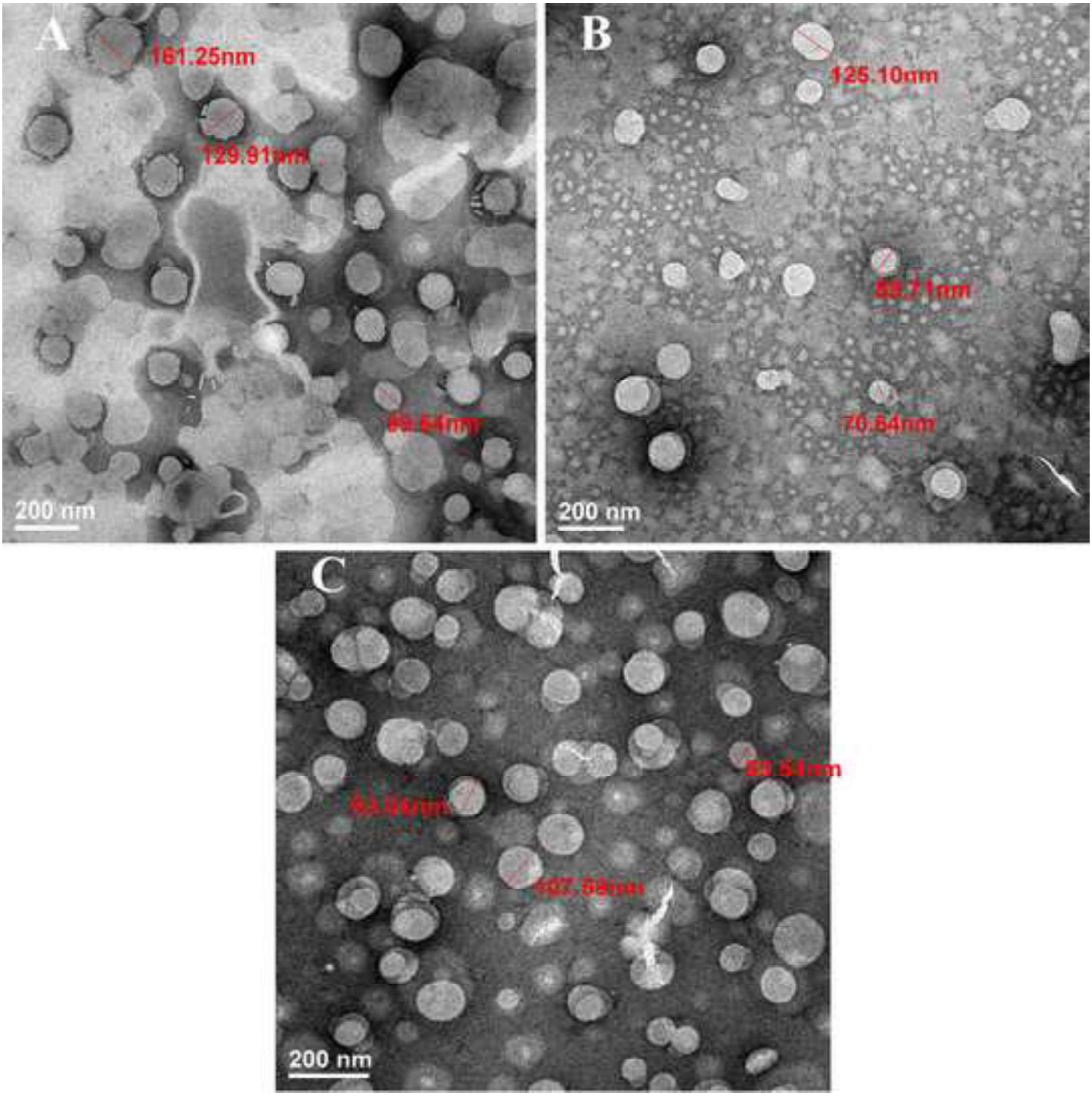

Fig.4

Click here to download high resolution image

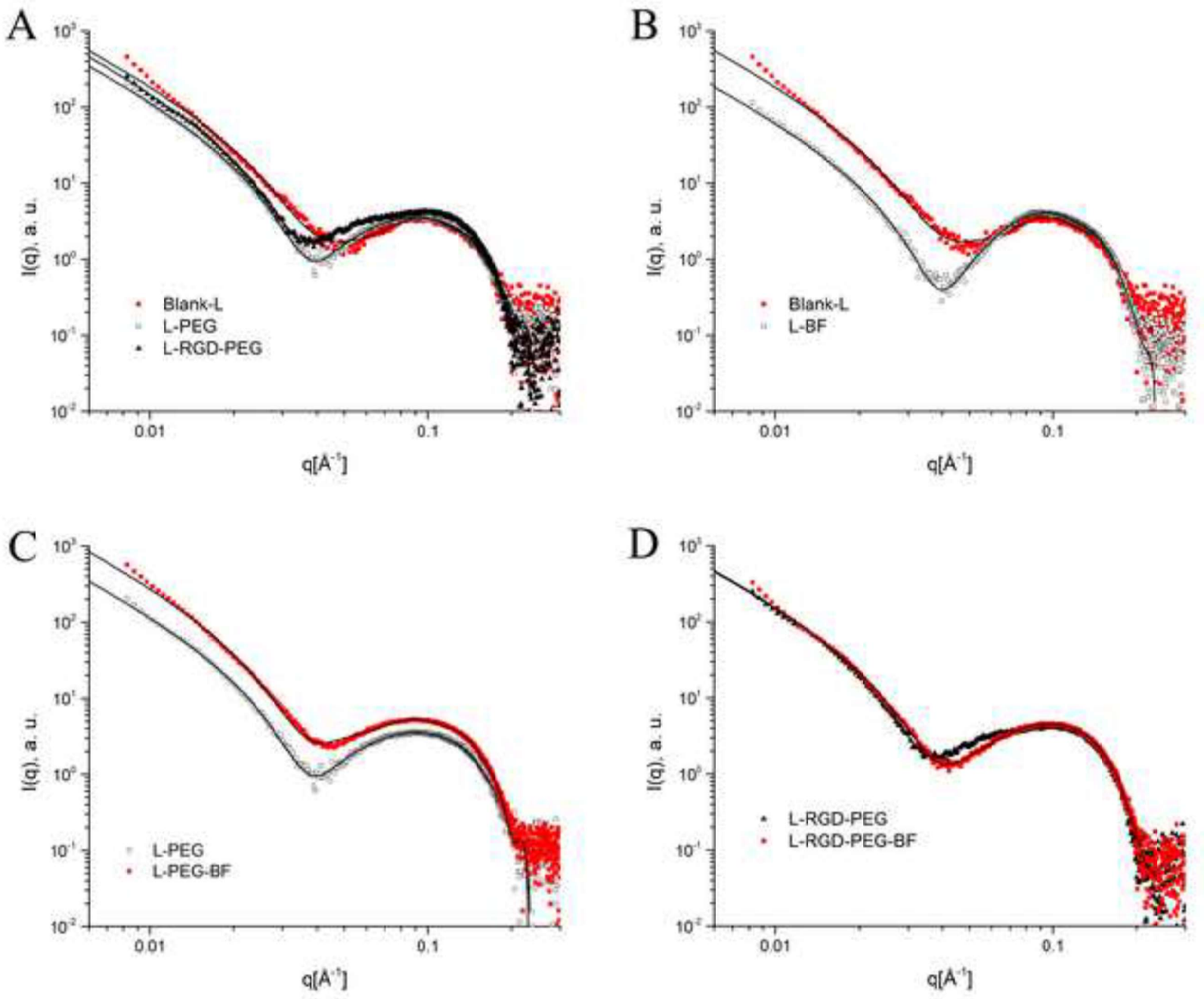

Fig.5

Click here to download high resolution image

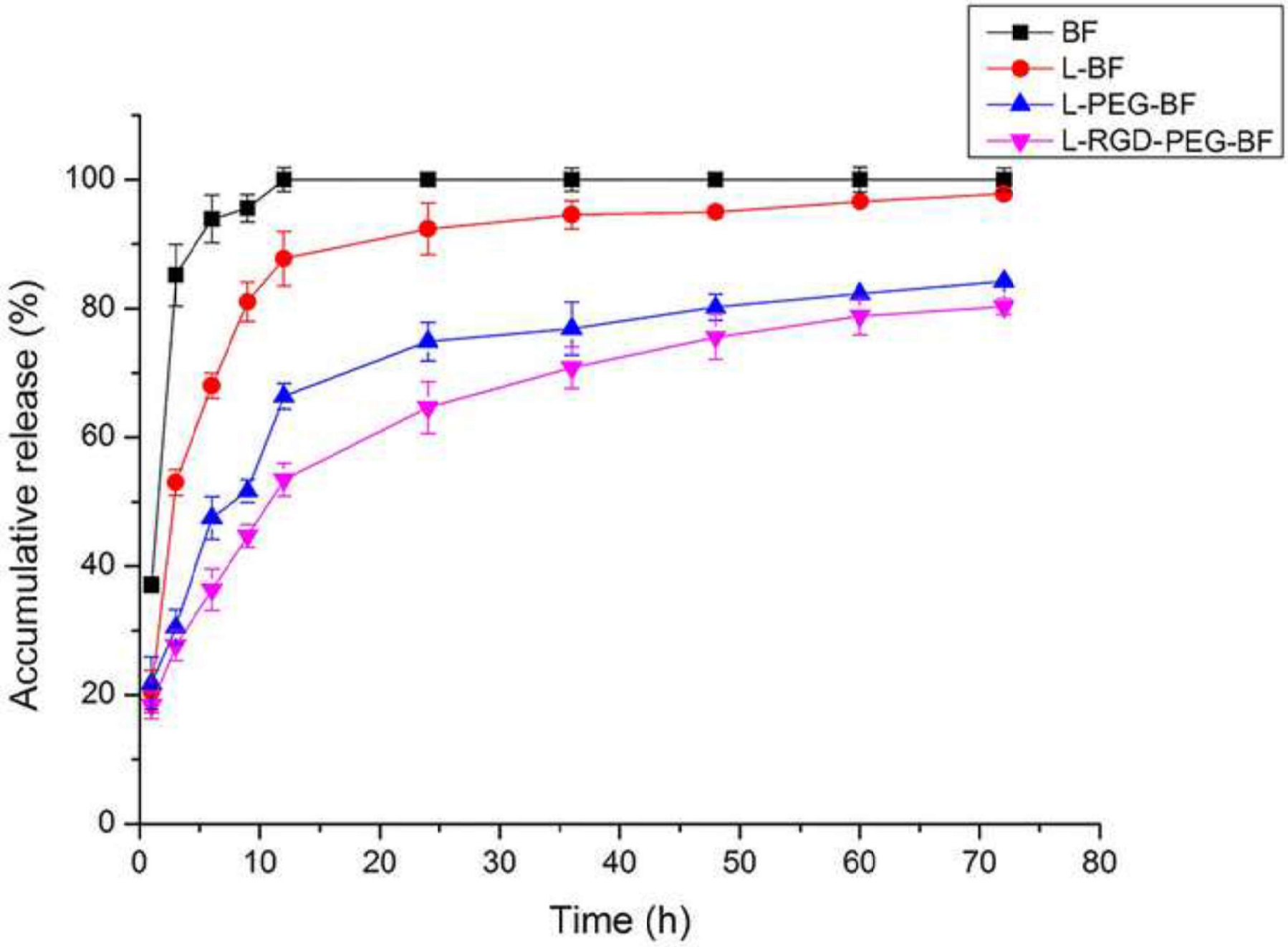

Fig.6

Click here to download high resolution image

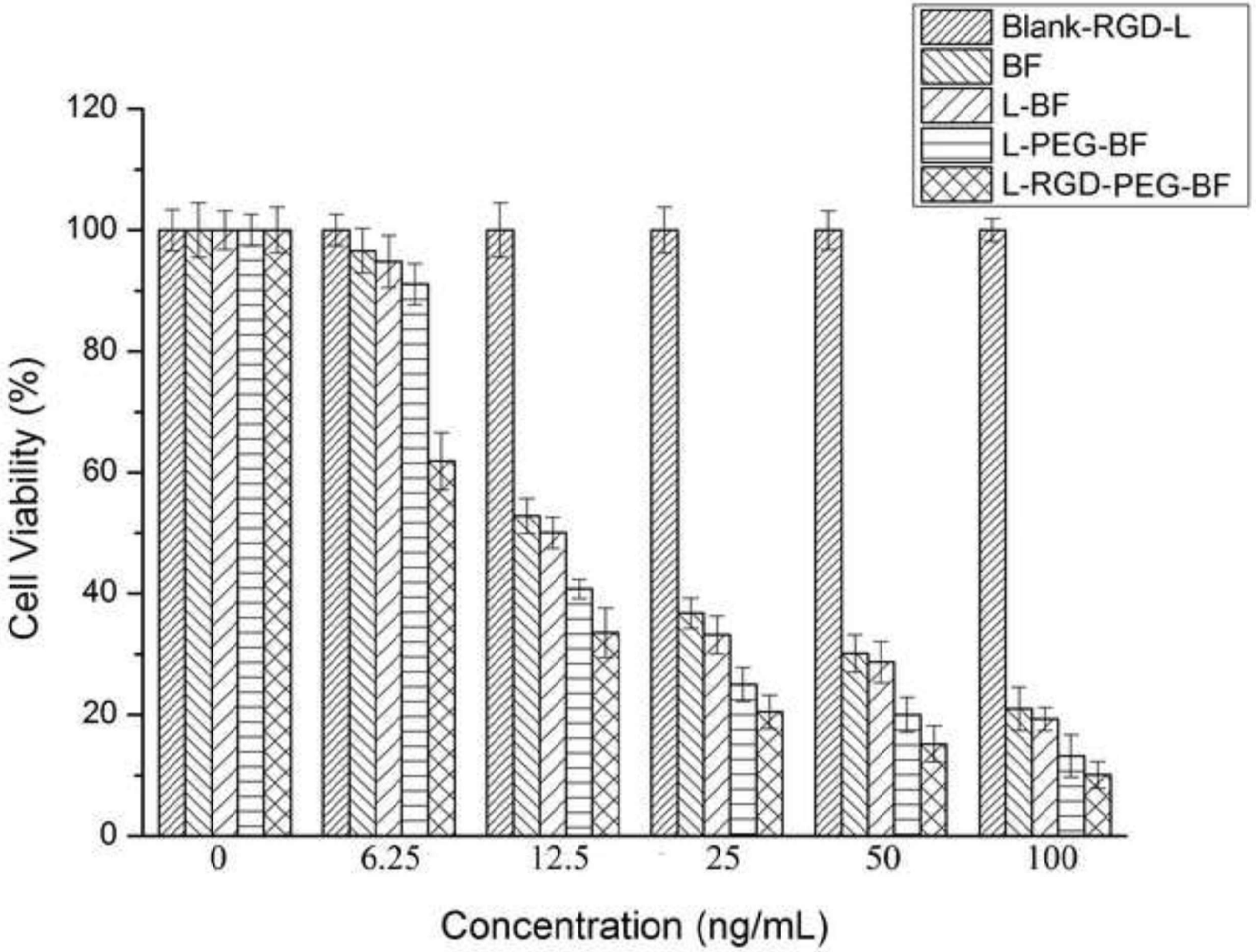

Fig.7

Click here to download high resolution image

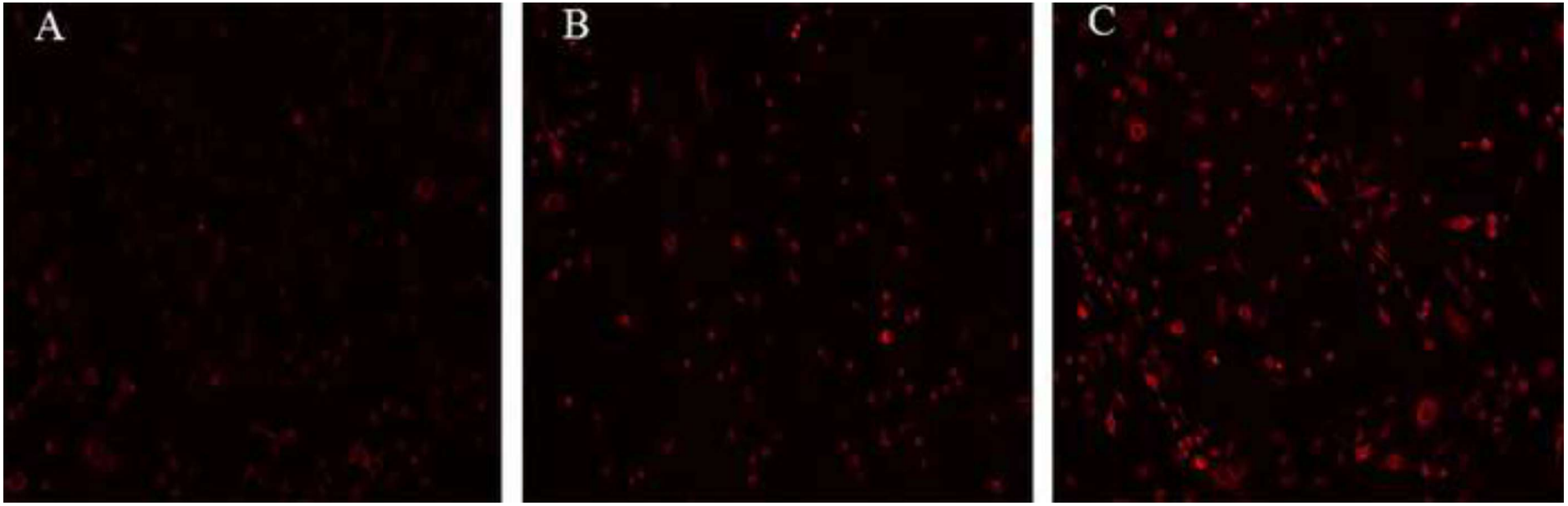

Fig.8

Click here to download high resolution image

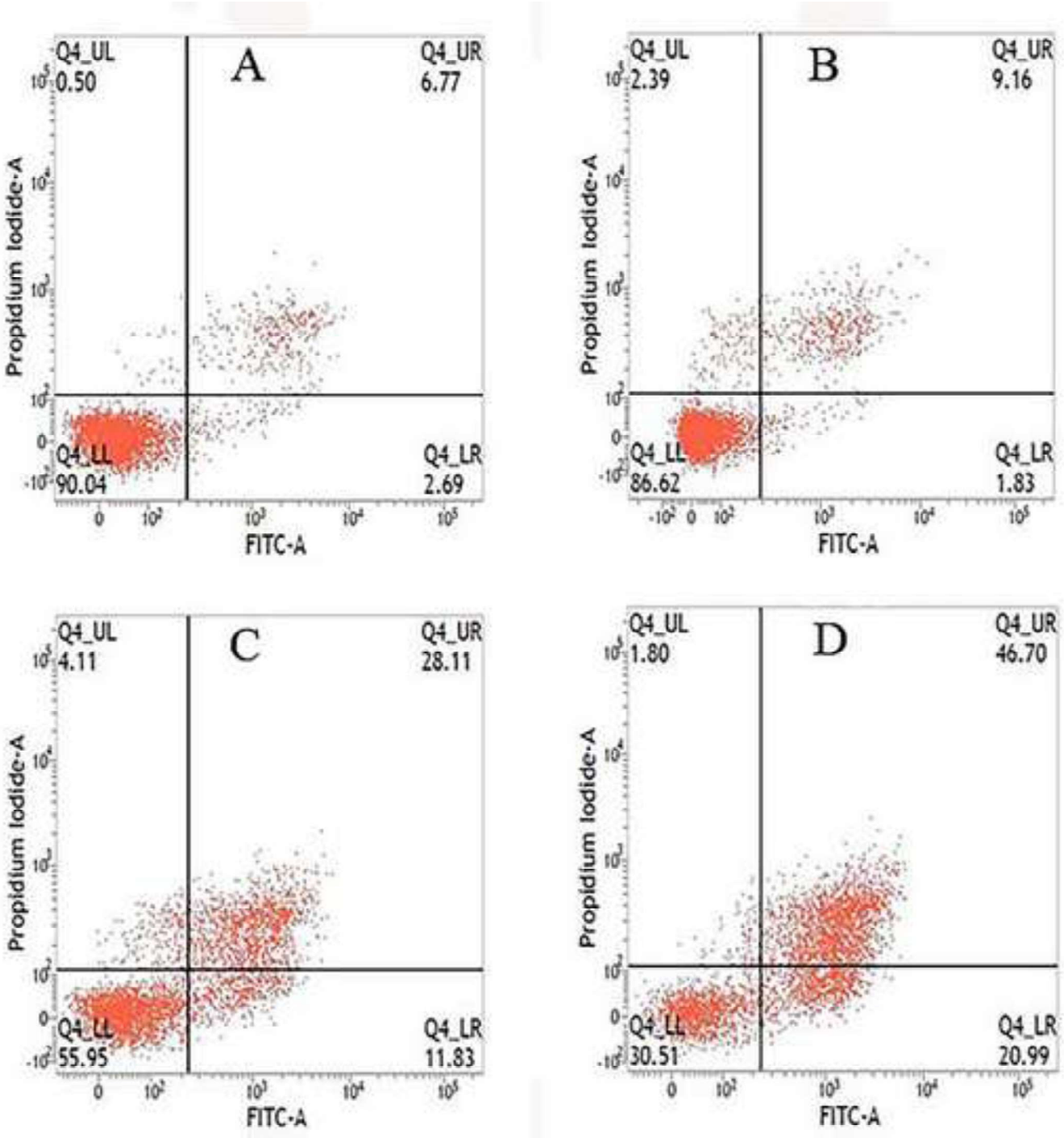

Supplementary Material

Click here to download Supplementary Material: Supplementary Material.docx